



GEOLOGY FOR SOCIETY

SINCE 1858



**GEOLOGICAL
SURVEY OF
NORWAY**

· NGU ·



Report no.: 2019.024		ISSN: 0800-3416 (print) ISSN: 2387-3515 (online)		Grading: Open	
Title: Georadar measurements at the Råbygda landslide site near Orkanger, Orkdal Municipality (February 16 th , 2019)					
Authors: Georgios Tassis, Louise Hansen, Inger-Lise Solberg			Client: NVE		
County: Trøndelag			Commune: Orkdal		
Map-sheet name (M=1:250.000) Trondheim			Map-sheet no. and -name (M=1:50.000) 1521-1 Orkanger		
Deposit name and grid-reference:			Number of pages: 25 Price (NOK): 130 Map enclosures:		
Fieldwork carried out: 01.03.2019		Date of report: 19.06.2019		Project no.: 368300	
				Person responsible: <i>Marco Brömmel</i>	
Summary: On February 16 th , 2019 a landslide took place at the Råbygda village just northwest of Orkanger, which resulted in a farmhouse destroyed and one human casualty. As a response to this situation, a multidisciplinary collaboration group was formed tasked to discern and report the causes of the landslide. NVE requested NGU's involvement in this collaboration and it was decided that a Ground Penetration Radar (GPR) survey should take place to help determine sediment thickness / depth to bedrock for the area and additionally suggest suitable geotechnical drilling positions. In this case, GPR was promoted as the main geophysical survey regardless of the fine-grained marine sediment coverage in the study area, due to their high content in silt as well as the presence of other coarser sediments. The area directly affected by the landslide was 90 meters long and 30 meters wide, but the GPR survey was decided to cover a larger area surrounding the landslide (200x200 meters). Eight profiles were planned with half of them following a southwest-northeast orientation while the other half was aligned perpendicularly (northwest-southeast). Fieldwork was carried out on a snowy day on March 1 st , 2019. Malå RTA (snake) system was utilized employing the 100 MHz antenna. The decision to use the snake system was based on the steep terrain and the speed at which such measurements would be fulfilled. The snow coverage was light on the surface, but the ground conditions were wet due to snow melting. In total, nine profiles were eventually measured covering a total distance of 1.6 kilometers. All profiles were tracked with the use of a Garmin GPSMAX 60Cx GPS for more accurate positioning while the standard hip-chain was used for signal triggering (traces every 0.25 meters). All assembled data were processed with the use of software package EKKO_Project v.4 and the initial results were presented with the use of an AGC gain filter in order to highlight all detected reflectors. Maximum depth penetration was up to 15 meters with a velocity of 0.1 m/ns. Based on these preliminary results, boreholes were drilled at suitable locations along the profiles until bedrock was found. Subsequently, all this information was plotted in the GPR profiles and based on these reference points, probable reflectors were interpreted as bedrock surface wherever this was possible using a DVL gain filter to only highlight the strongest reflectors. Finally, all depth to bedrock estimations and measurements i.e. GPR interpretations and boreholes were gridded to create a 2D map of the sediment thickness distribution in the study area.					
Keywords:		Geophysics		Georadar	
Bedrock		Sediments		Landslide	
Fjord-marine		Fjord valley		Valley fill	

CONTENTS

- 1. INTRODUCTION 7
- 2. FIELDWORK AT REITAN 7
- 3. WORKFLOW / DATA HANDLING 9
- 4. METHOD, APPLICATION AND PROCESSING 9
 - 4.1 General..... 9
 - 4.2 The GPR survey at Reitan..... 10
- 5. RESULTS 15
- 6. DEPTH TO BEDROCK 24
- 7. CONCLUSION 25
- 8. ACKNOWLEDGEMENTS 25
- 9. REFERENCES 25

FIGURES

- Figure 2.1: GPR measurement across the landslide pit. 8
- Figure 2.2: Light snow coverage outside the landslide scar (increasing uphill). 8

- Figure 4.1: Positioning for Georadar profiles collected in Reitan (yellow & red) and drillholes opened after the survey (cyan). 14

- Figure 5.1: Processed image for profile Re01-495 with the use of an AGC (top) and a DVL (bottom) gain function. Red boxes indicate bedrock depth from drillings and purple dotted line subsequent interpretation. 16
- Figure 5.2: Processed image for profile Re02-496 with the use of an AGC (top) and a DVL (bottom) gain function. Red boxes indicate bedrock depth from drillings and purple dotted line subsequent interpretation. 17
- Figure 5.3: Processed image for profile Re03-497 with the use of an AGC (top) and a DVL (bottom) gain function. Red boxes indicate bedrock depth from drillings and purple dotted line subsequent interpretation. 18
- Figure 5.4: Processed images for profiles Re04a-498 and Re04b-499 with the use of an AGC (top) and a DVL (bottom) gain function. Red boxes indicate bedrock depth from drillings and purple dotted line subsequent interpretation. 19
- Figure 5.5: Processed image for profile Re05-503 with the use of an AGC (top) and a DVL (bottom) gain function. Red boxes indicate bedrock depth from drillings and purple dotted line subsequent interpretation. 20
- Figure 5.6: Processed image for profile Re06-502 with the use of an AGC (top) and a DVL (bottom) gain function. Red boxes indicate bedrock depth from drillings and purple dotted line subsequent interpretation. 21
- Figure 5.7: Processed image for profile Re07-501 with the use of an AGC (top) and a DVL (bottom) gain function. Red boxes indicate bedrock depth from drillings and purple dotted line subsequent interpretation. 22
- Figure 5.8: Processed image for profile Re08-500 with the use of an AGC (top) and a DVL (bottom) gain function. Red boxes indicate bedrock depth from drillings and purple dotted line subsequent interpretation. 23

Figure 6.1: Depth to bedrock based on GPR interpretations and drillings. 24

TABLES

Table I: Profile Re01-495 – Length: 236 meters. 10
Table II: Profile Re02-496 – Length: 164 meters. 11
Table III: Profile Re03-497 – Length: 200 meters 11
Table IV: Profile Re04a-498 – Length: 135 meters..... 11
Table V: Profile Re04b-499 – Length: 117 meters..... 11
Table VI: Profile Re05-503 – Length: 179 meters..... 12
Table VII: Profile Re06-502 – Length: 183 meters..... 12
Table VIII: Profile Re07-501 – Length: 188 meters..... 12
Table IX: Profile Re08-500 – Length: 181 meters..... 12
Table X: Modules employed in EKKO_project v.4 for GPR processing 13

1. INTRODUCTION

On February 16th, 2019 a landslide took place at the farm Reitan in Råbygd village just northwest of Orkanger, which resulted in a farmhouse destroyed and one human casualty. As a response to this situation, a multidisciplinary collaboration group with members from NTNU (lead), NVE, NGI and NGU was formed and tasked to investigate and elucidate the causes of the landslide. NVE requested NGU's involvement in this collaboration and it was decided that a Ground Penetrating Radar (GPR) survey should take place to help determine sediment thickness and/or depth to bedrock for the area and additionally suggest suitable geotechnical drilling positions. It should be noted that this report will only focus on bedrock interpretation with the use of GPR. More detailed interpretation including layering within the overburden is presented in other reports of this project.

In this case, GPR was promoted as the main geophysical survey method despite the known marine sediment coverage in the study area. Marine sediments like clay normally hinder the penetration of the electromagnetic pulse that the Georadar transmits in the ground and therefore GPR surveys are not advisable in such areas. However, the high content in silt as well as the knowledge of other coarser sediments below marine sediments in the area could offer more suitable conditions for Georadar measurements.

2. FIELDWORK AT REITAN

The area directly affected by the landslide was 90 meters long and 30 meters wide, but the GPR survey was decided to cover a larger area surrounding the landslide (200x200 meters). Eight profiles were planned with half of them following the southwest-northeast direction while the other half was aligned perpendicularly (northwest-southeast).

Fieldwork was carried out on a snowy day on March 1st, 2019. Malå RTA (snake) system was utilized employing the 100 MHz antenna. The decision to use the snake system was based on the high inclination of the terrain and the speed at which such measurements would be fulfilled. The snow coverage was light on the surface, but the ground conditions were wet due to snow melting (**figure 2.1**). In total, nine profiles were eventually measured covering a total distance of 1.6 kilometers. All profiles were tracked with the use of a Garmin GPSMAX 60Cx GPS for more accurate positioning while the standard hip-chain was used for signal triggering (traces every 0.25 meters).



Figure 2.1: GPR measurement across the landslide pit.



Figure 2.2: Light snow coverage outside the landslide scar (increasing uphill).

3. WORKFLOW / DATA HANDLING

All assembled data were processed with the use of software package EKKO_Project v.4 and the initial results were presented with the use of an AGC gain filter in order to highlight all detected reflectors. Maximum depth penetration was up to 15 meters with a velocity of 0.1 m/ns. Based on these preliminary results, boreholes were drilled at suitable locations along the profiles until bedrock was found.

Subsequently, all this information was plotted in the GPR profiles and based on these reference points, probable reflectors were interpreted as bedrock surface wherever this was possible using a DVL gain filter to only highlight the strongest reflectors. Finally, all depth to bedrock estimations and measurements i.e. GPR interpretations and boreholes were gridded to create a 2D map of the sediment thickness distribution in the study area. It should be noted that the fact that geophysics preceded drilling, is the proposed procedure in all similar cases by NGU.

NGU's responsibility concerning the geophysical survey planned, was to collect, process and interpret the GPR data collected in the landslide site as presented in this report.

4. METHOD, APPLICATION AND PROCESSING

4.1 General

Ground Penetrating Radar (GPR) or Georadar as is also commonly mentioned, is an electromagnetic geophysical technique which can be used to investigate stratification in the underground. It uses electromagnetic fields to probe lossy dielectric materials to detect structures and changes in material properties within the materials (Davis & Annan,1989). With GPR, the electromagnetic fields propagate as essentially nondispersive waves. The signal emitted travels through the material, is scattered and/or reflected by changes in impedance, giving rise to events which appear similar to the emitted signal (Butler, 2005). These reflected signals are registered at the surface and utilized to reconstruct interfaces in the ground. This is achieved by the compilation images where 1D electromagnetic "soundings" are positioned consecutively to create a uniform 2D image (radargram).

In lossy dielectric materials, electromagnetic fields can only penetrate to a limited depth before being absorbed. Hence, exploration depth is always a variable. However, the frequency range where GPR functions is between 1 and 1000 MHz, and the choice of frequency also controls the projected depth of an investigation. In lower frequencies, the pulses are easily dispersed while at higher frequencies the signal absorption becomes too strong and the penetration depth extremely limited. GPR studies are therefore planned with a frequency choice that compromises penetration depth (lower frequencies) with desired signal resolution (higher frequencies) in relation to the survey goals.

4.2 The GPR survey at Reitan

For the measurements in the survey area (Reitan), the system employed was Malå RTA (Snake) due to the slush, steep and uneven ground conditions inside the landslide pit and the surrounding farming fields. This system utilizes a parallel endfire antenna configuration (antennas in a row) which allows flexibility in rough terrain conditions but also produces a slightly inferior signal compared to the classic perpendicular broadside configuration (antennas parallel). However, it has been discerned that the expected deterioration in data quality is not prohibitive when inaccessible areas such as the landslide area in Reitan can be surveyed with the Snake system (Tassis et al., 2015).

Based on the assessment that the sediment coverage in the area is no thicker than a few meters, the 100 MHz antenna frequency was picked for utilization. This particular frequency offers a projected penetration which is deep enough for this study area and a detail level high enough so that more information about the internal sediment structure can be potentially revealed. Trace spacing was set equal to 0.25 meters, time window equal to 600 ns i.e. 30 meters depth coverage on a default 0.1 m/ns velocity and triggering was prompted by the standard hip-chain of the instrument. Positioning was obtained using a Garmin GPSMAP 60Cx handheld GPS by marking each starting and ending position of each profile and by recording our route in between these points.

Figure 4.1 shows the positioning of the profiles measured in Reitan as well as the drilling points which followed the Georadar survey. There were nine profiles measured, covering a total distance of 1.6 kilometers along two directions, one along the SSW to NNE direction and perpendicular to the extension of the landslide pit (profiles Re05 to Re08) and a second along the NNW to SSE direction i.e. parallel to the extension of the landslide (profiles Re01 to Re04a & b). Profile Re02 was measured along the axis of the landslide pit while the landslide itself begins just south of the profile's intersection with profile Re06 and continues all the way downslope. It should be noted that the second part of the profile naming is referring to the code assigned to each profile when saved on the internal memory of the instrument and is used as an index to the system's library. Positioning for each profile is shown in **tables I to IX** in UTM zone 32N coordinates and in meters.

Easting UTM 32N (meters)	Northing UTM32N (meters)
540830	7021516
540814	7021530
540770	7021559
540739	7021581
540712	7021596
540677	7021622
540652	7021647
540643	7021658

Table I: Profile Re01-495 – Length: 236 meters.

Easting UTM 32N (meters)	Northing UTM32N (meters)
540599	7021647
540609	7021634
540635	7021613
540653	7021604
540663	7021598
540672	7021588
540688	7021567
540718	7021550
540723	7021546

Table II: Profile Re02-496 – Length: 164 meters.

Easting UTM 32N (meters)	Northing UTM32N (meters)
540730	7021508
540713	7021523
540677	7021558
540650	7021571
540615	7021599
540596	7021615
540575	7021632

Table III: Profile Re03-497 – Length: 200 meters

Easting UTM 32N (meters)	Northing UTM32N (meters)
540571	7021625
540609	7021568
540613	7021514
540615	7021504

Table IV: Profile Re04a-498 – Length: 135 meters.

Easting UTM 32N (meters)	Northing UTM32N (meters)
540633	7021522
540643	7021509
540667	7021466
540701	7021429

Table V: Profile Re04b-499 – Length: 117 meters.

Easting UTM 32N (meters)	Northing UTM32N (meters)
540717	7021683
540700	7021665
540649	7021631
540591	7021592
540570	7021581

Table VI: Profile Re05-503 – Length: 179 meters.

Easting UTM 32N (meters)	Northing UTM32N (meters)
540575	7021563
540587	7021572
540634	7021599
540678	7021634
540726	7021664

Table VII: Profile Re06-502 – Length: 183 meters.

Easting UTM 32N (meters)	Northing UTM32N (meters)
540751	7021641
540733	7021622
540699	7021582
540690	7021579
540670	7021557
540615	7021518

Table VIII: Profile Re07-501 – Length: 188 meters.

Easting UTM 32N (meters)	Northing UTM32N (meters)
540631	7021495
540658	7021511
540703	7021539
540714	7021550
540764	7021590
540778	7021600

Table IX: Profile Re08-500 – Length: 181 meters.

Processing took place with the use of EKKO_project v.4 software. For this purpose, ReflexW v. 7 was used to convert all Malå files into a format which is readable by EKKO_project. Additionally, EKKO_project uses the standard GPGSA format files for positioning and these had to be prepared as well. In order to do so, the handheld GPS measured points were extrapolated to match the number of traces for each Georadar profile and then topography for each trace was sampled from digital elevation models available for the study area. It must be noted here that the scanned morphology of the landslide pit was made available to us and therefore, all traces were assigned the

correct elevation value i.e. scanned topography after the landslide event in the affected area and LiDAR elevation everywhere else.

Processing module	Value / Description
<i>Repick First Break</i>	<i>Average ~ 20 ns</i>
<i>Dewow</i>	<i>Window Width (Pulse Widths): 1.33</i>
<i>Background Subtraction</i>	<i>Filter Width: 20 m (rectangular)</i>
<i>Bandpass Filter 100 MHz</i>	<i>Fc1 40 % / Fp1 80 % / Fp2 120 % / Fc2 160 %</i>
<i>1st Run: AGC Gain</i>	<i>Level 4 / Window Width: 1 m / Maximum Gain: 500 ns</i>
<i>2nd Run: DVL Gain</i>	<i>Level 5 / Alpha: 1.00 / Beta: 0.40</i>
<i>Velocity</i>	<i>0.1 m/ns</i>

Table X: Modules employed in EKKO_project v.4 for GPR processing.

The original processing routine utilized a straightforward approach and all intermediate steps are presented in **table X**. It should be noted here that during the first processing run, an AGC gain function was used purposefully for all detected reflectors to be highlighted and therefore give a better outlook as to where test drilling should be done. On the second processing run and after proposed drilling was carried out in Reitan, a DVL gain function was used instead to differentiate the strongest reflectors and help with bedrock surface interpretation.

Georadar survey at landslide near Orkanger

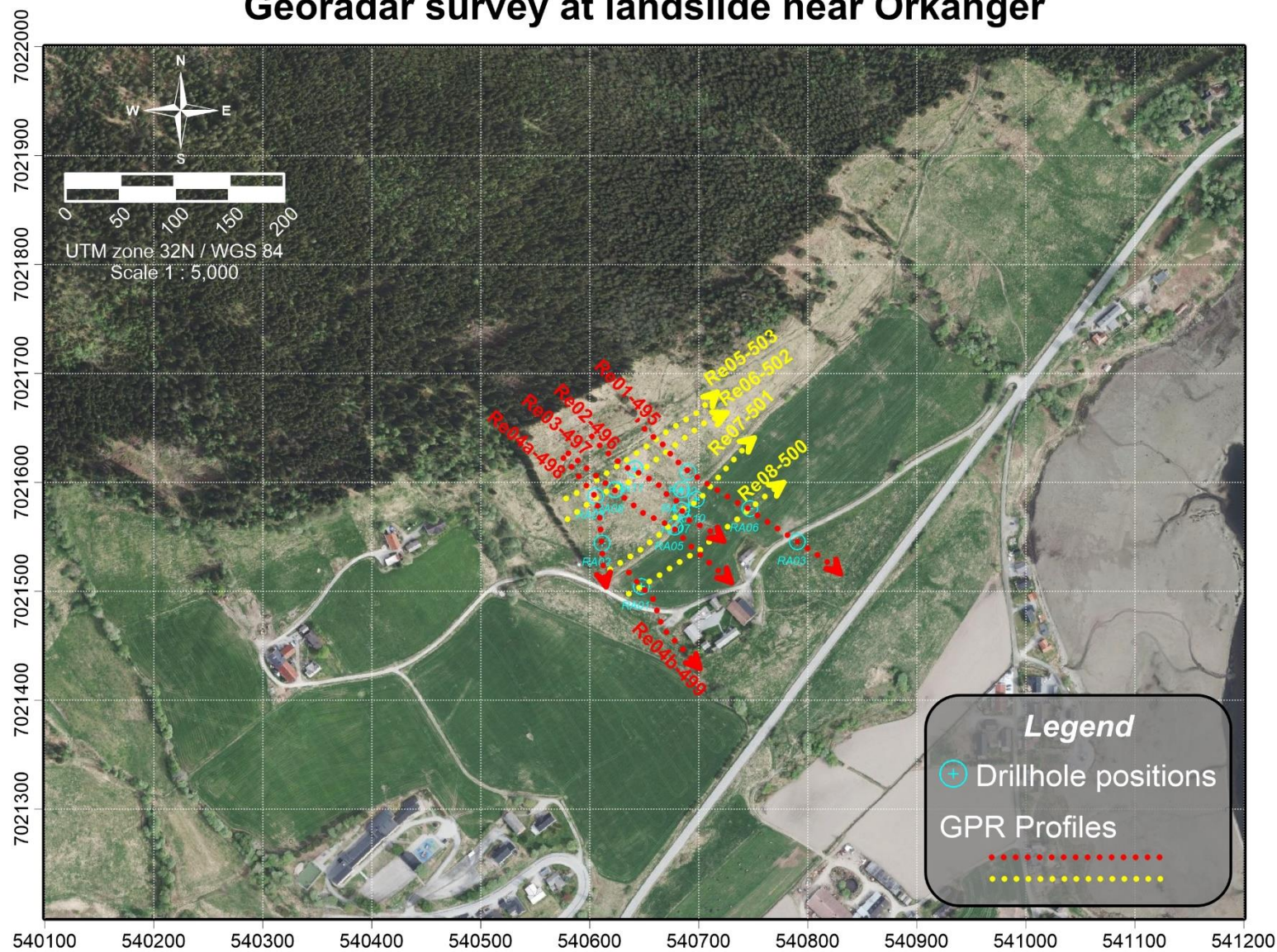


Figure 4.1: Positioning for Georadar profiles collected in Reitan (yellow & red) and drillholes opened after the survey (cyan).

5. RESULTS

In this section we will present the GPR processing results for all profiles. **Figures 5.1 to 5.8** present two different versions for profiles 1 to 8 (or Re01-495 to Re08-500). The version shown at the top of each figure represents the processing done prior to drilling and/or interpretation and utilized an AGC gaining function which accentuates all reflectors detected in each line. At the bottom, the processing shown consists of the same routines (see **table X**) but with a DVL gaining function which only highlights the most pronounced reflectors in each profile. Combined with the drilling results which are incorporated in the same DVL results and marked with red squares, interpretations have been made on possible bedrock topography by L. Hansen and I.L. Solberg. These interpretations are plotted with purple dotted lines and they are only found where reflection patterns could be associated and followed in relation with drillings. Lastly, other helpful features appearing in the figures are cross-points with other profiles shown with black crosses and elevation before the landslide took place shown with a red dotted line only to the profiles where this applies.

Our results indicate that the study area offers different penetration depths locally, according to the composition of the ground beneath. Therefore, there are localities where the 100 MHz antenna reaches down to 15 meters while in other places the penetrations depth is limited to less than 5 meters which is indicative of either clay materials and/or strong presence of water. Another interesting feature is that when examining the profiles running SW to NE (**figures 5.5 to 5.8**), local topographic lows present clearly deeper signal penetration which could be linked to materials brought to the slope and placed to smoothen topography for farming purposes. **Figure 5.2** which represents the profile running along the axis of the landslide, presents the highest and most consistent depth penetration throughout its length. In this profile, it can be marked that drilling and subsequent interpretation show a thicker overburden northwest of the landslide which is then almost halved beneath the affected area towards the southeast.

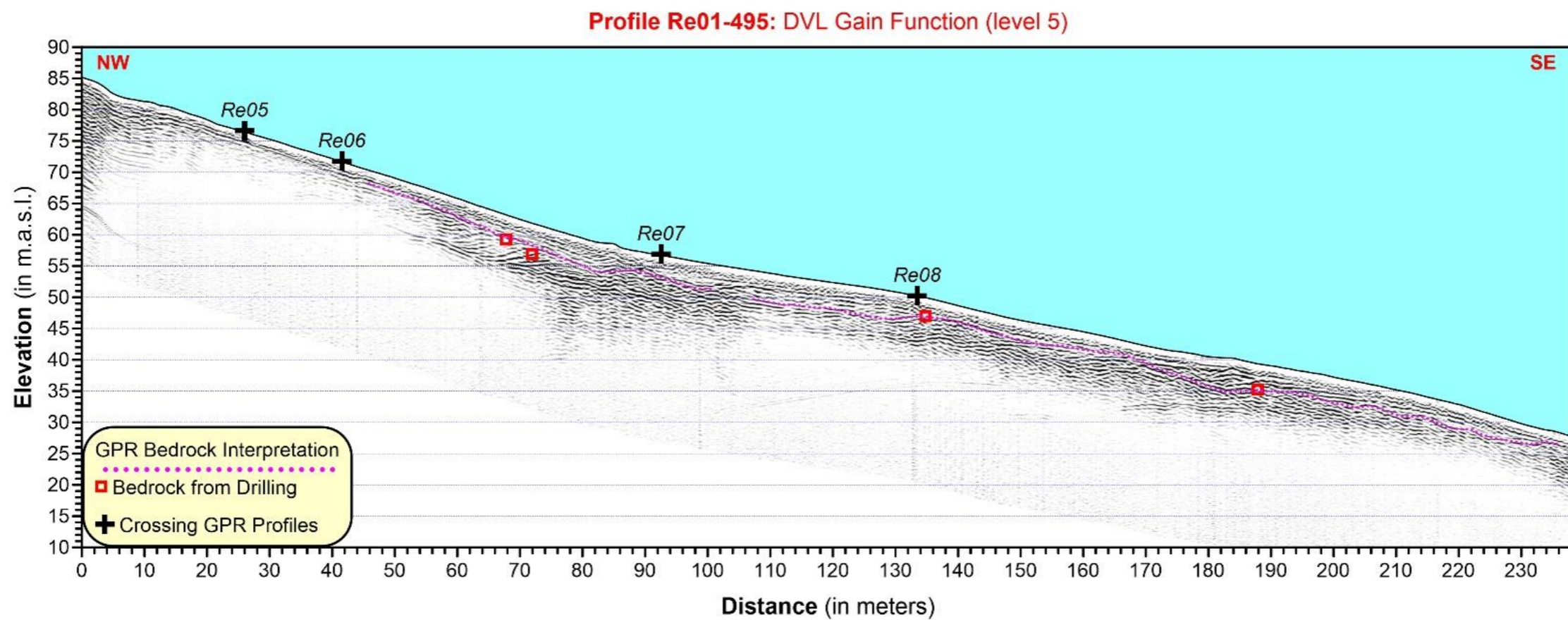
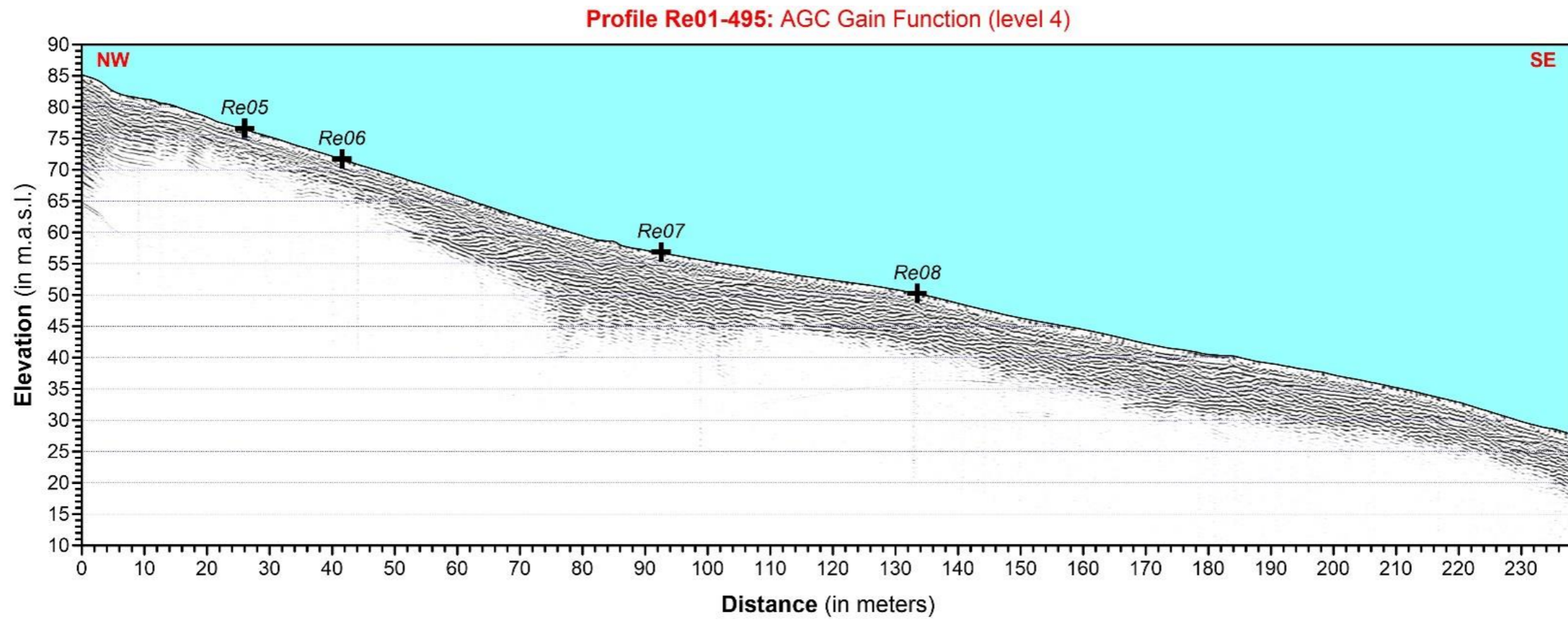


Figure 5.1: Processed image for profile Re01-495 with the use of an AGC (top) and a DVL (bottom) gain function. Red boxes indicate bedrock depth from drillings and purple dotted line subsequent interpretation.

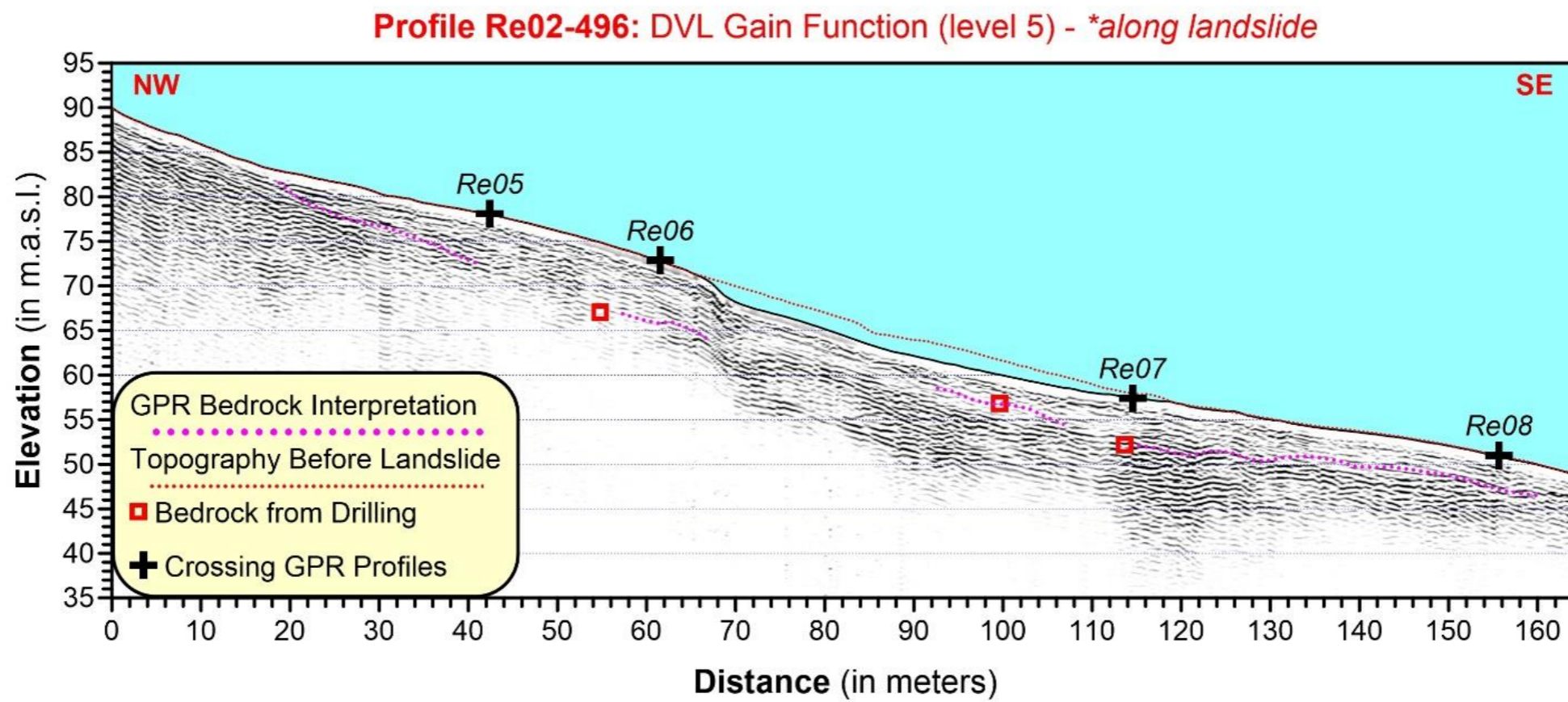
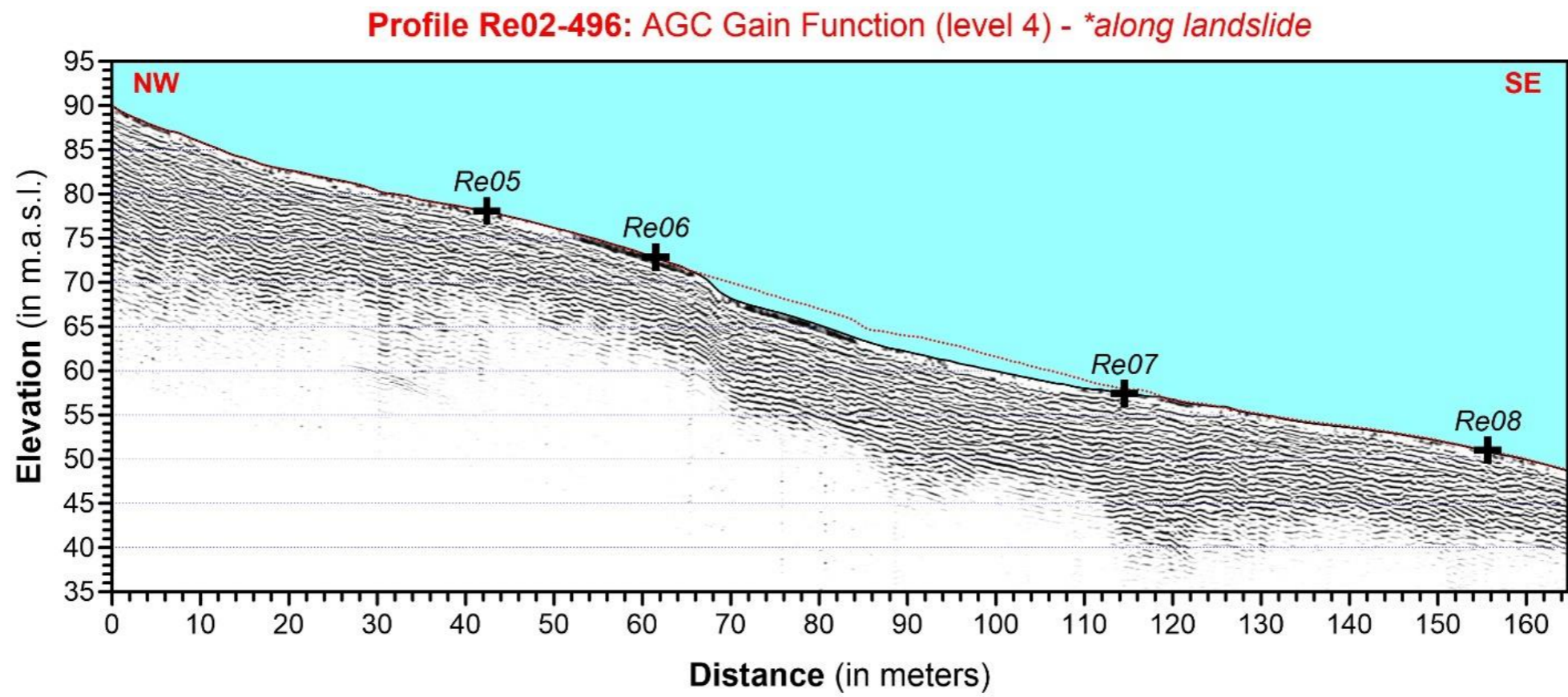


Figure 5.2: Processed image for profile Re02-496 with the use of an AGC (top) and a DVL (bottom) gain function. Red boxes indicate bedrock depth from drillings and purple dotted line subsequent interpretation.

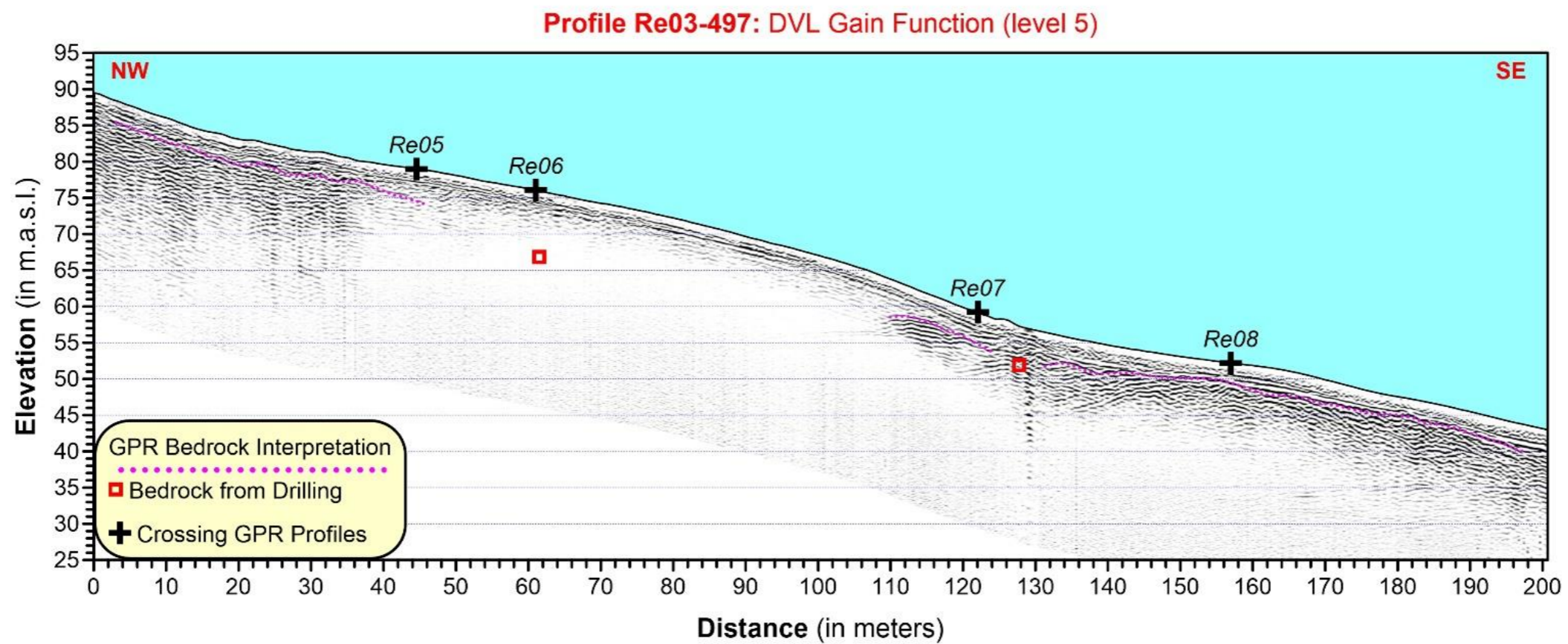
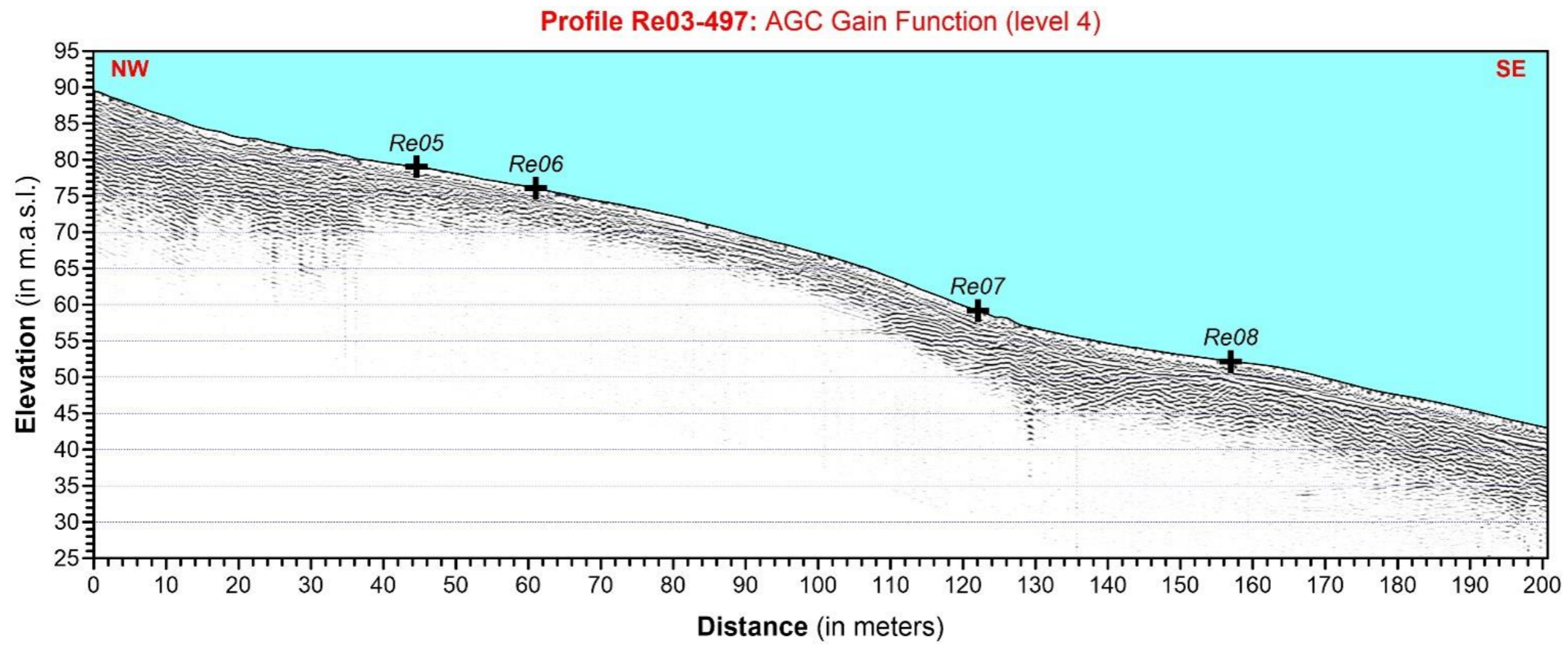


Figure 5.3: Processed image for profile Re03-497 with the use of an AGC (top) and a DVL (bottom) gain function. Red boxes indicate bedrock depth from drillings and purple dotted line subsequent interpretation.

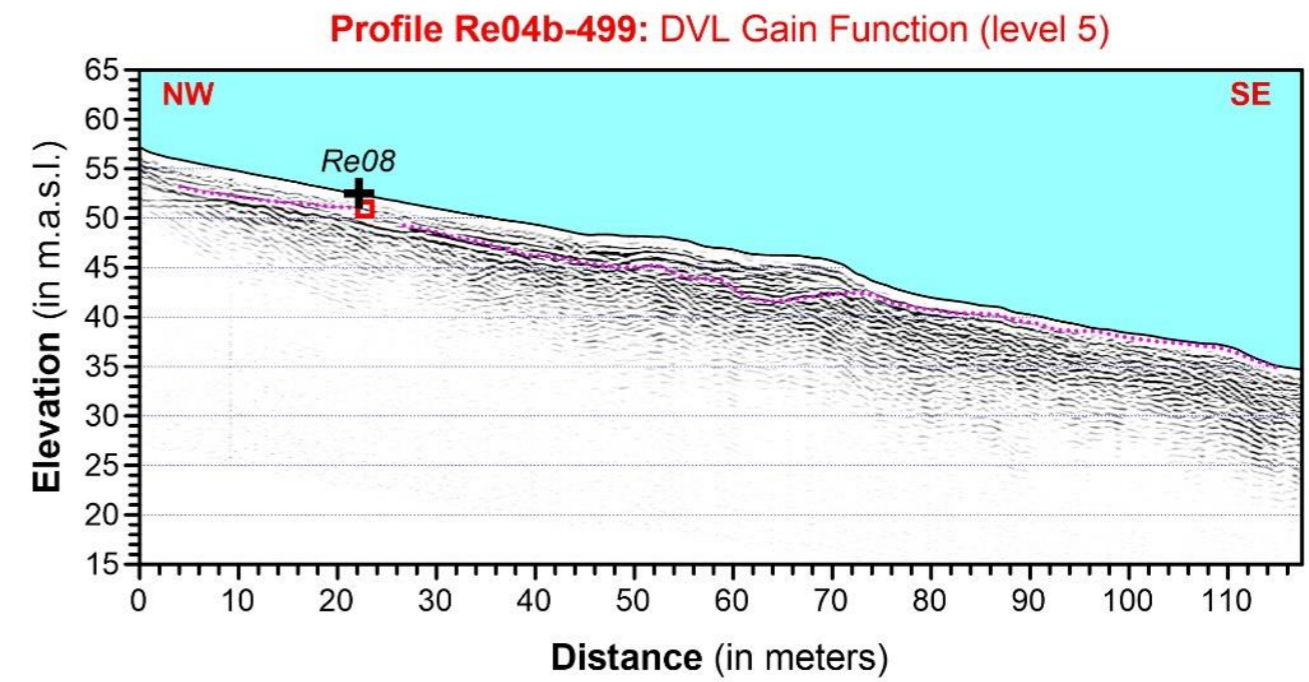
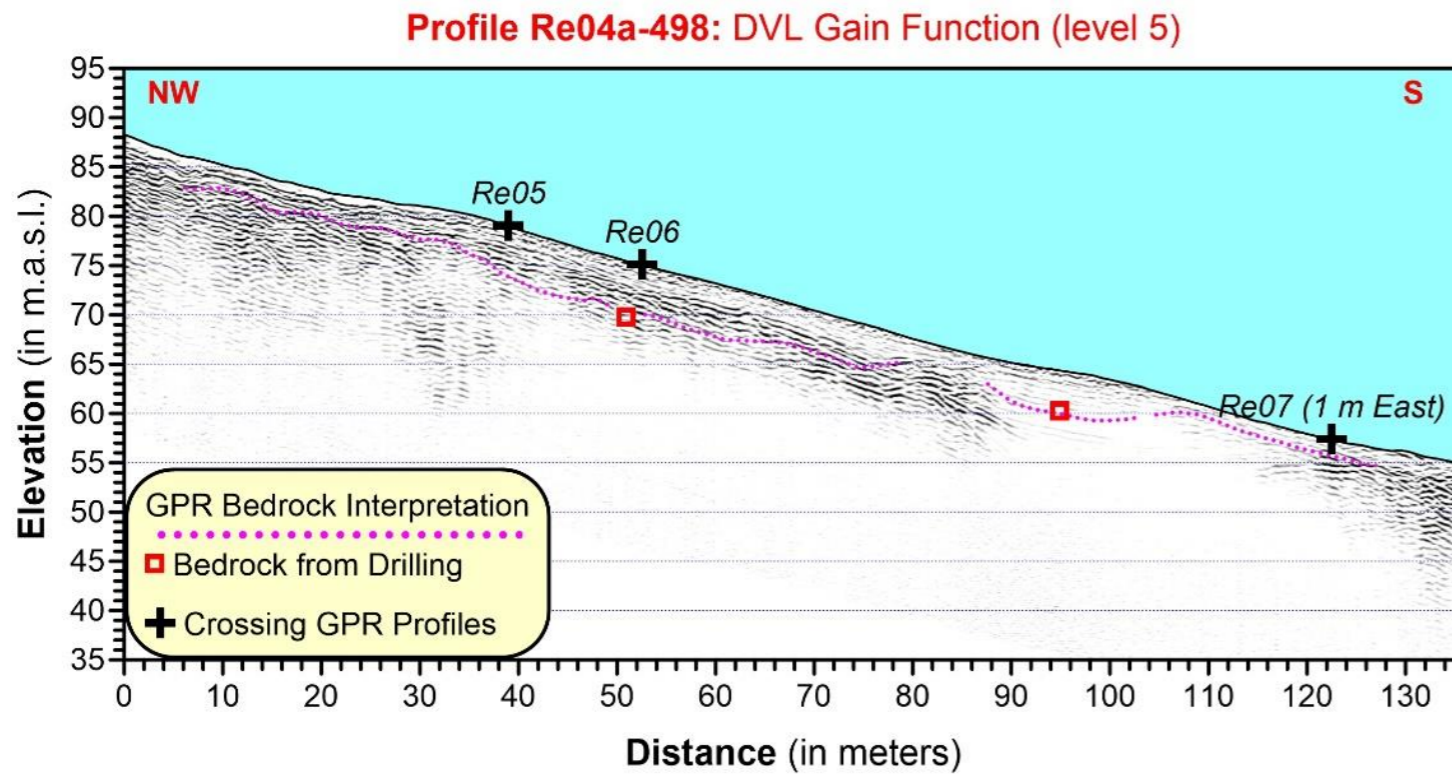
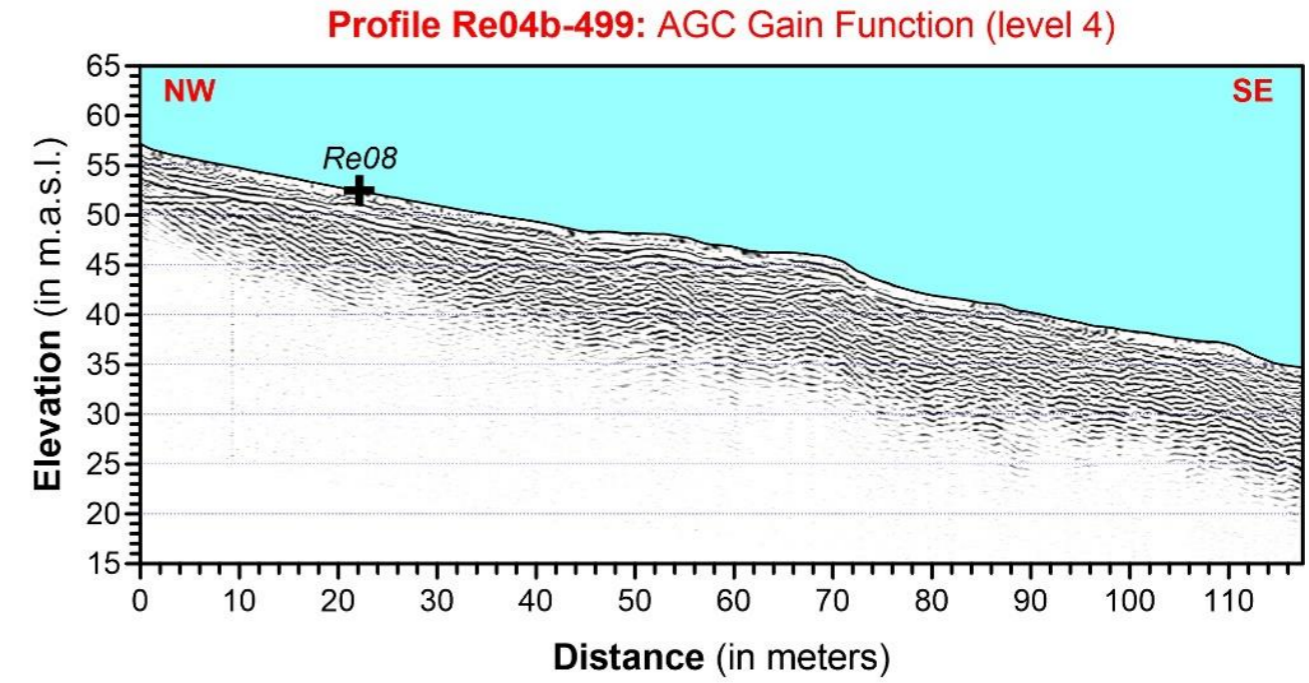
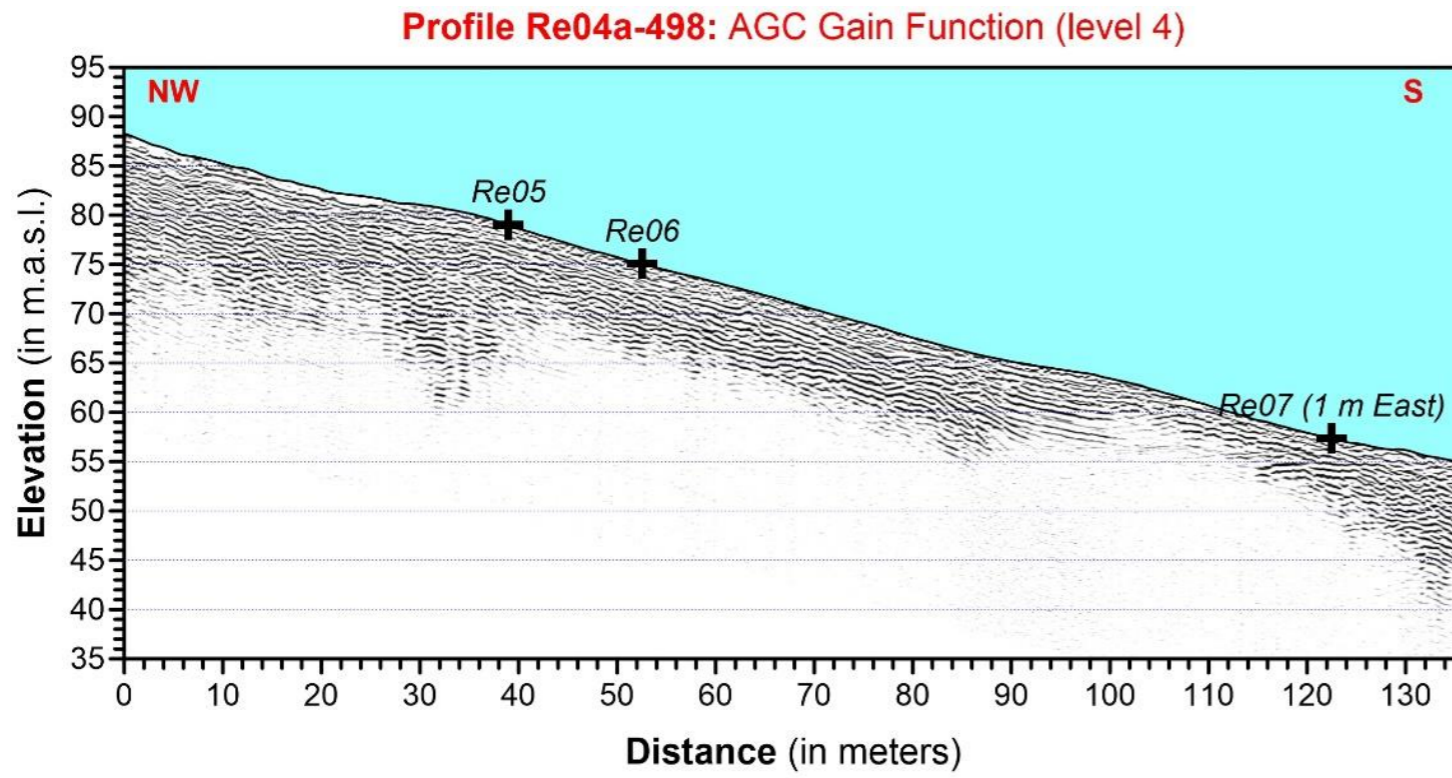
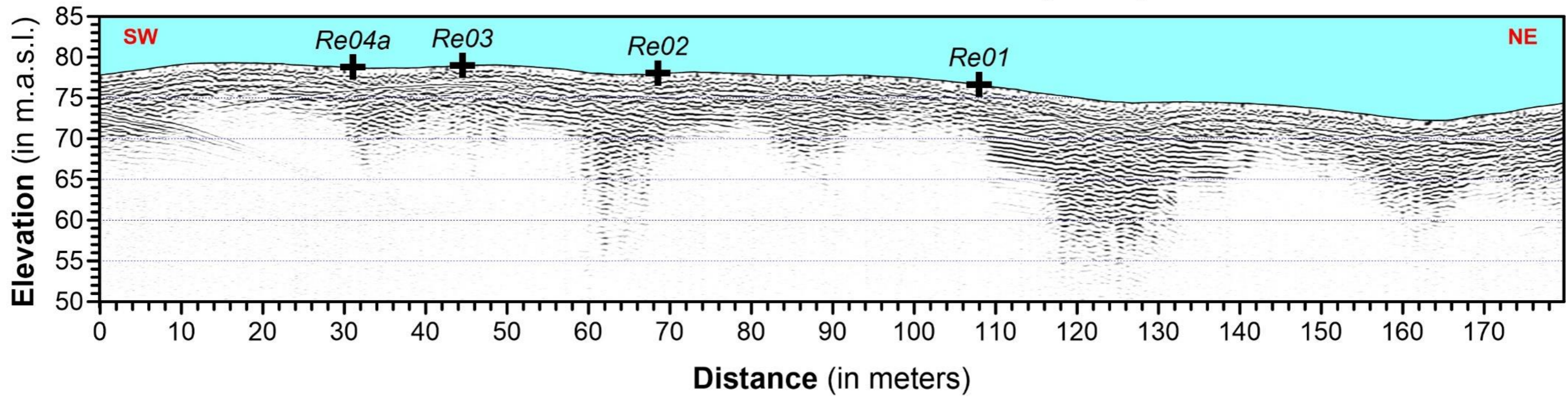


Figure 5.4: Processed images for profiles Re04a-498 and Re04b-499 with the use of an AGC (top) and a DVL (bottom) gain function. Red boxes indicate bedrock depth from drillings and purple dotted line subsequent interpretation.

Profile Re05-503: AGC Gain Function (level 4)



Profile Re05-503: DVL Gain Function (level 5)

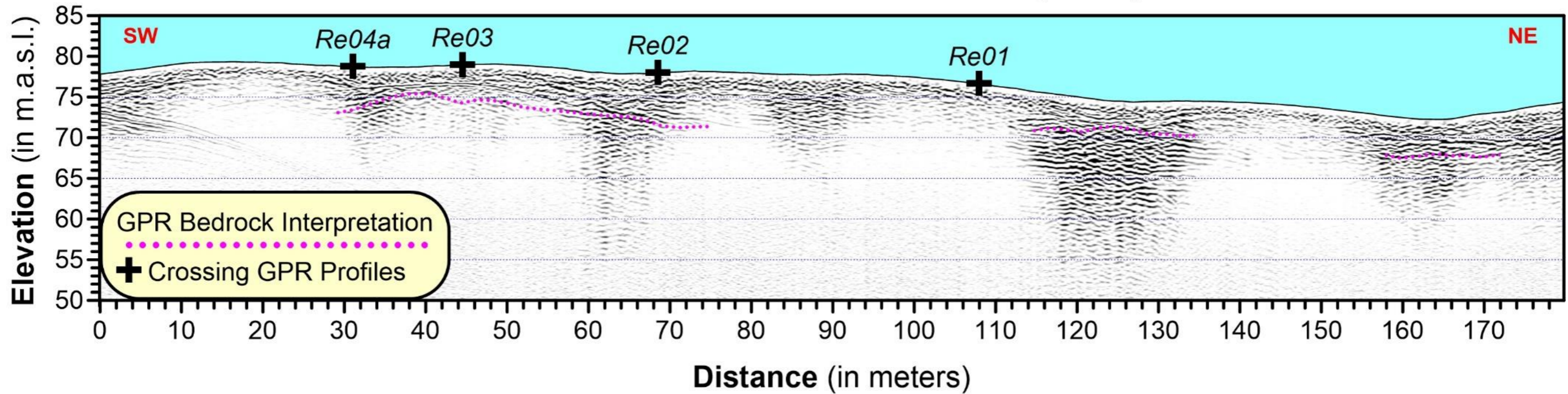


Figure 5.5: Processed image for profile Re05-503 with the use of an AGC (top) and a DVL (bottom) gain function. Red boxes indicate bedrock depth from drillings and purple dotted line subsequent interpretation.

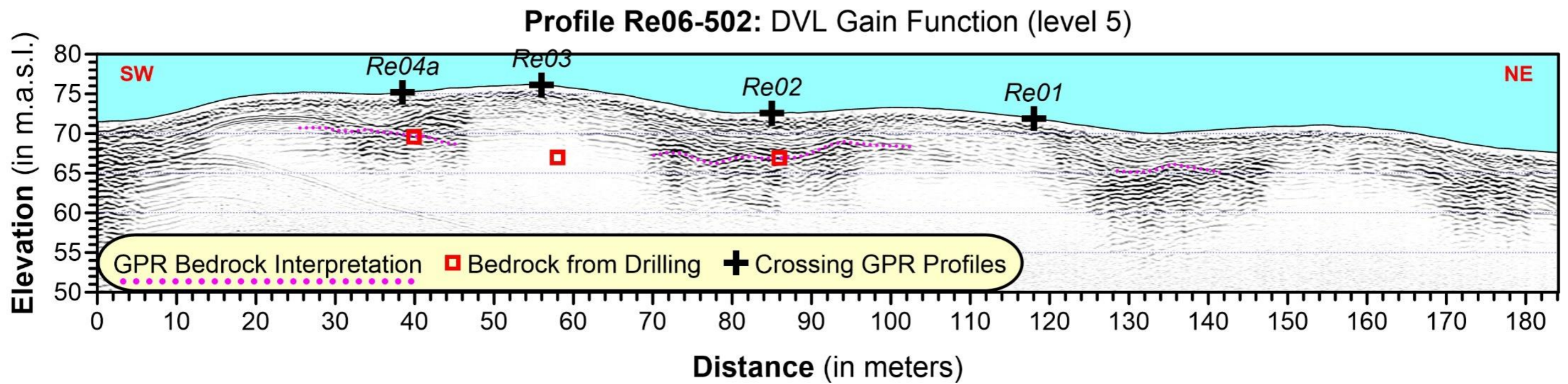
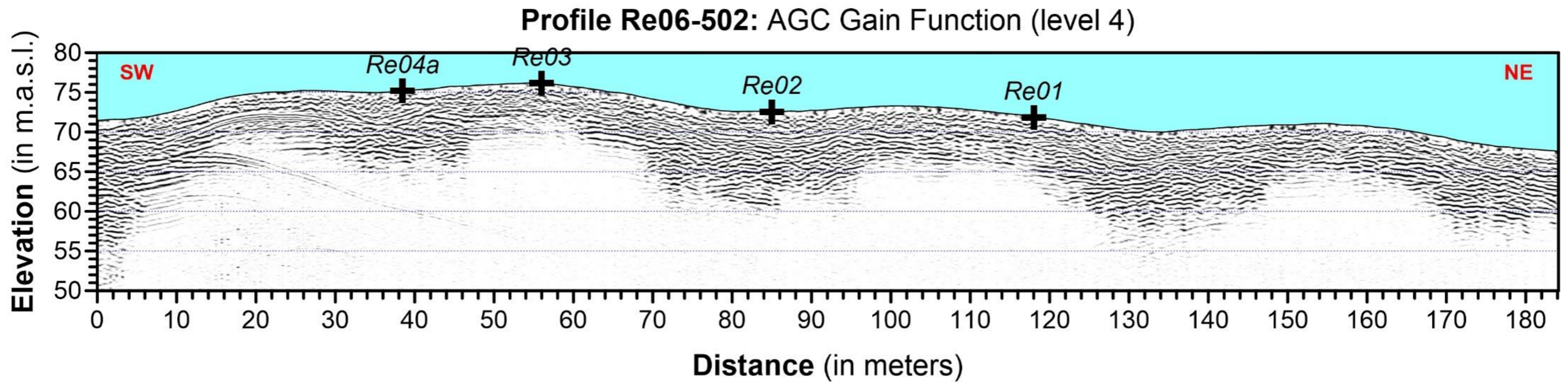
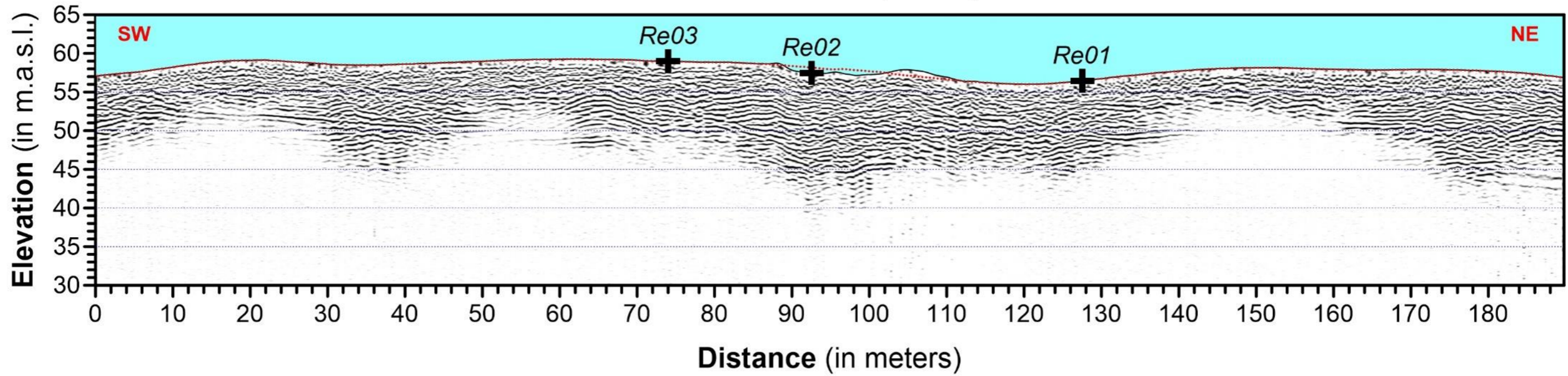


Figure 5.6: Processed image for profile Re06-502 with the use of an AGC (top) and a DVL (bottom) gain function. Red boxes indicate bedrock depth from drillings and purple dotted line subsequent interpretation.

Profile Re07-501: AGC Gain Function (level 4) - *across mid landslide



Profile Re07-501: DVL Gain Function (level 5) - *across mid landslide

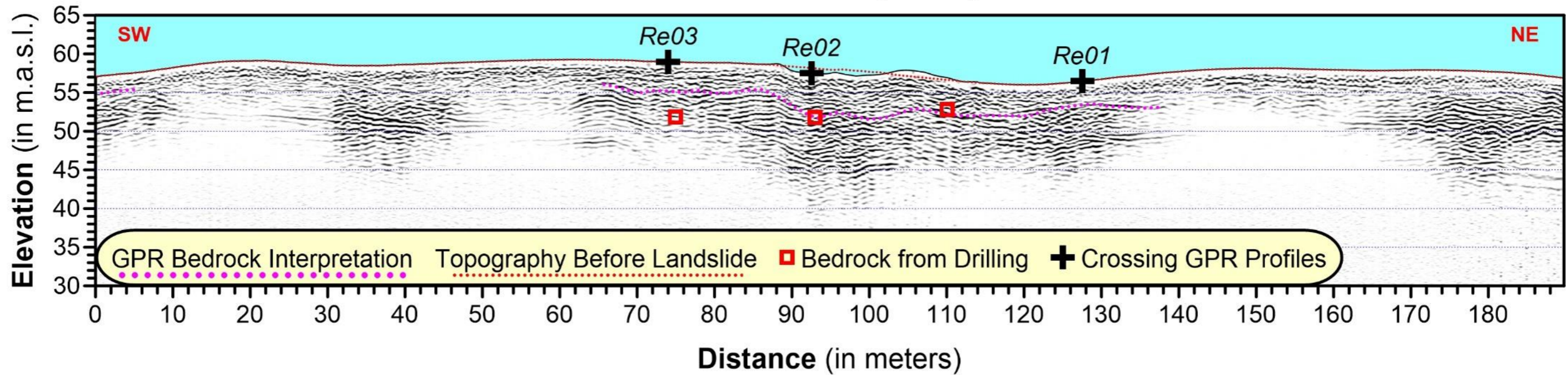


Figure 5.7: Processed image for profile Re07-501 with the use of an AGC (top) and a DVL (bottom) gain function. Red boxes indicate bedrock depth from drillings and purple dotted line subsequent interpretation.

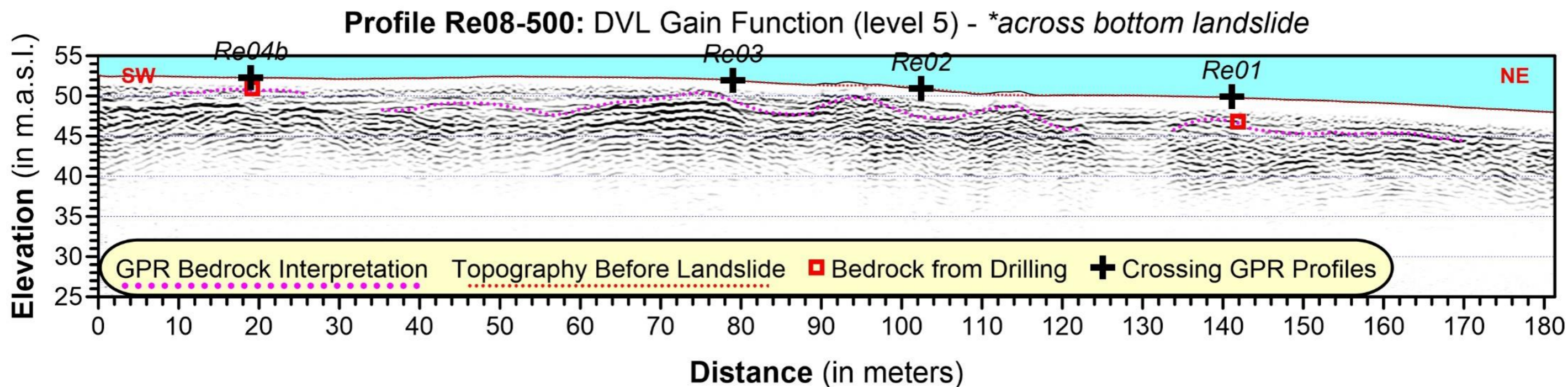
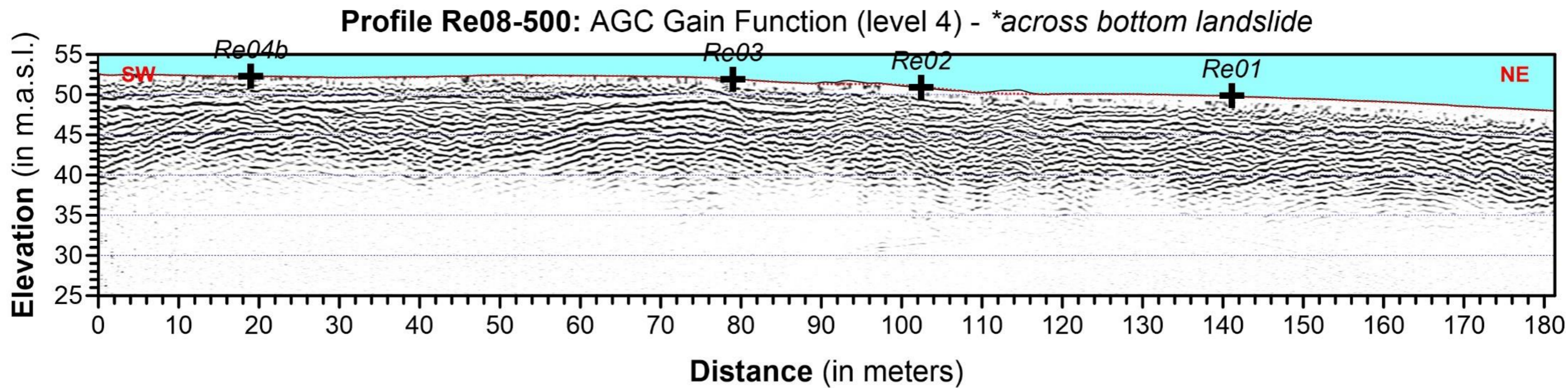


Figure 5.8: Processed image for profile Re08-500 with the use of an AGC (top) and a DVL (bottom) gain function. Red boxes indicate bedrock depth from drillings and purple dotted line subsequent interpretation.

6. DEPTH TO BEDROCK

In order to obtain a better understanding of the bedrock topography in the study area after the landslide as extracted by GPR measurements aided by drilling, all interpretations shown in **figures 5.1 to 5.8** were extracted and then assigned UTM coordinates. Then, all georeferenced interpretation points together with the drilling information were unified in a file and subsequently gridded to create an outlook of the overburden thickness (depth to bedrock) for the entire area shown in **figure 6.1**. It should be noted that since interpretation (small white circles) and drilling points (pink crosses) are scarce, gridding was done using a large interval (15 m – Kriging method) which led to a rather low-resolution end result. However, this gridding can help draw useful conclusions regarding the geographic distribution of depth to bedrock in the study area.

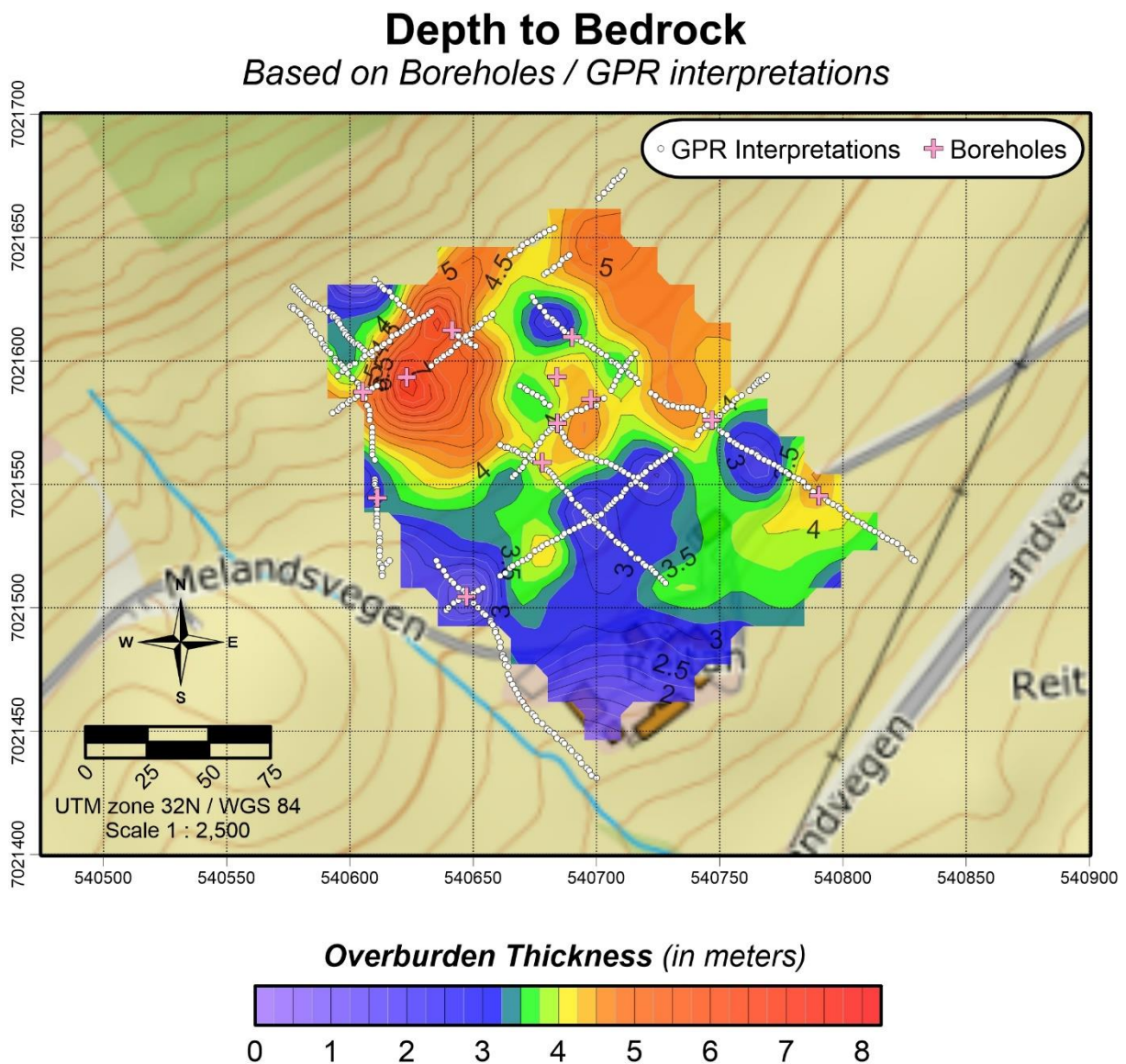


Figure 6.1: Depth to bedrock based on GPR interpretations and drillings.

According to **figure 6.1**, depth to bedrock distribution in Reitan roughly splits the study area in two subareas, one to the north which presents a higher overburden thickness (four meters or more) and one to the south which is characterized by shallower bedrock (four meters or less). This limit is following the UTM zone 32 N northing at 7 021 550 meters and it shows that the transition from deeper to shallower bedrock takes place quite rapidly. Exceptions to this rough subdivision can be found in both subareas: bedrock is almost outcropping at the northwest corner of the grid and at another pronounced and isolated locality near the northeast edge while two “valleys” of thicker overburden layers can be seen both east and west of the landslide affected area. Concerning the landslide itself, the decrease in overburden thickness is evident in the area of the landslide scar while this setting appears to be similar to the west of the landslide too. Generally, the depth to bedrock obtains its maximum value mainly at the northwest but also at the northeast part of the grid too.

7. CONCLUSION

In conclusion, GPR application in this project has again proved the method to be extremely useful, fast and efficient. The fact that ground geophysics preceded drilling helped both parties i.e. suitable drilling positions were based on the preliminary GPR results and subsequently drilling results helped interpretations on the final processing results. As a result, a low-resolution but highly informative 2D map was produced which successfully visualizes the depth to bedrock distribution in the wider area.

8. ACKNOWLEDGEMENTS

We would like to thank senior engineer Radmil Popovic from the Institute of Geography at NTNU for lending us their 100 MHz Malå RTA antenna to conduct the survey since our 100 MHz antenna was not available due to ongoing repairs.

9. REFERENCES

- Butler, D.K. (edited), 2005: Near Surface Geophysics (Investigations in Geophysics No. 13). Society of Exploration Geophysicists, ISBN: 1-56080-130-1 (Volume - 756 pp.).
- Davis, J.L., and Annan, A.P., 1986: Borehole radar sounding in CR-6, CR-7 and CR-8 at Chalk River, Ontario: Technical Record TR-401, Atomic Energy of Canada Ltd.
- Tassis, G., Rønning, J.S., Hansen, L. and Tønnesen, J.F., 2015: Comparison between Sensors & Software and Malå GPR equipment based on test measurements at Bøaøyna, Stryn Municipality, Norway. NGU Report 2015.014 (41 pp.).



GEOLOGICAL
SURVEY OF
NORWAY

· NGU ·

Geological Survey of Norway
PO Box 6315, Sluppen
N-7491 Trondheim, Norway

Visitor address
Leiv Eirikssons vei 39
7040 Trondheim

Tel (+ 47) 73 90 40 00
E-mail ngu@ngu.no
Web www.ngu.no/en-gb/